Cooperative Resonances in Light Scattering from Two-Dimensional Atomic Arrays

Ephraim Shahmoon,[1] Dominik S. Wild,[1] Mikhail D. Lukin,[1] and Susanne F. Yelin[1,2]
[1]*Department of Physics, Harvard University, Cambridge Massachusetts 02138, USA*
[2]*Department of Physics, University of Connecticut, Storrs, Connecticut 06269, USA*
(Received 1 October 2016; revised manuscript received 2 February 2017; published 14 March 2017)

We consider light scattering off a two-dimensional (2D) dipolar array and show how it can be tailored by properly choosing the lattice constant of the order of the incident wavelength. In particular, we demonstrate that such arrays can operate as a nearly perfect mirror for a wide range of incident angles and frequencies, and shape the emission pattern from an individual quantum emitter into a well-defined, collimated beam. These results can be understood in terms of the cooperative resonances of the surface modes supported by the 2D array. Experimental realizations are discussed, using ultracold arrays of trapped atoms and excitons in 2D semiconductor materials, as well as potential applications ranging from atomically thin metasurfaces to single photon nonlinear optics and nanomechanics.

DOI: 10.1103/PhysRevLett.118.113601

Control over propagation and scattering of light fields plays a central role in optical science. In particular, it is well known that emitters exhibit a strongly modified optical response on resonance. For example, enhanced optical scattering in 2D arrays of linearly polarizable elements have been extensively studied in photonics [1–5]. Recently, it has been shown that thin 2D metamaterials, known as metasurfaces, whose constituent elements are optical antennas with varying resonances, can drastically alter the transmitted field by enabling spatial control of its amplitude, phase and polarization [6,7]. As a rule, these elements are microfabricated from macroscopic material, while the separation between the array elements is typically much smaller than the operating wavelength. At the same time, resonant light can be completely reflected by individual atoms when they are strongly coupled to nanophotonic devices with subwavelength localization of light [8–12]. Intuitively, this originates from resonant enhancement of the optical cross section of a polarizable dipole, which at resonance universally scales as λ^2, λ being its resonant wavelength. Such single atom reflectors yield extraordinary nonlinearities at the level of individual photons [13–15].

Here we explore light scattering from a 2D ordered and dilute array of atoms, with a lattice constant of the order of a wavelength, as can be realized, e.g., using ultracold atoms loaded into optical lattices [16,17]. In such a case near-resonant operation can still lead to strong scattering. Indeed, vanishing transmission at normal incidence was recently discovered in a numerical study of 2D atomic lattices for a specific frequency and lattice arrangement [18]. Because of resonant enhancement, one may naïvely expect that a single layer of dipoles, even if they are as small as individual atoms, may "tile" the plane and thus act as a strong scatterer, provided the density of dipoles exceeds $1/\lambda^2$ [Fig. 1(a)]. This reasoning, though providing intuition for the possibility of strong scattering in dilute media, ignores the important effect of multiple scattering of electromagnetic fields between the dipoles, associated with dipole-dipole interactions [19–24]. These interactions are crucial to explain the collective phenomena and their tunability explored in this work.

In what follows, we develop an analytical approach to the scattering problem, highlighting the role of the *cooperative resonances* of the dipolar array and their associated collective surface-wave excitations. Strong scattering generically occurs when the frequency of the incident light matches that of the cooperative resonance. The control of scattering off the array can be achieved by adjusting the lattice constant, which determines the cooperative resonances via the underlying dipolar interactions. We demonstrate that the array can

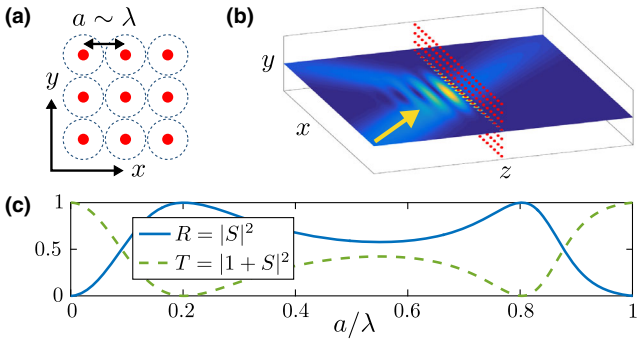

FIG. 1. (a) 2D array of atoms spanning the xy plane at $z = 0$, with interatomic spacing a on the order of the resonant wavelength of the atoms, λ. For resonant light, the individual atomic cross section is of order λ^2 (dashed circles). (b) Light scattering off the array in the single diffraction order regime: The incident field (yellow arrow) produces a forward scattered field at $z > 0$ and a reflected field at $z < 0$. (c) Intensity transmission coefficient T and reflection coefficient R for a square lattice at normal incident and resonant light ($\delta = 0$) as a function of the lattice constant a. Strong scattering is observed with perfect reflection occurring at $a/\lambda \approx 0.2, 0.8$.

form a nearly perfect mirror at almost all incident angles, as well as act as an efficient coupler between an emitter and a collimated optical mode. These results open a new direction in the possibility to mold the flow of light, namely, by using atomically thin metasurfaces.

Scattering at normal incidence.—We consider a 2D array of identical pointlike particles with a generic linear and isotropic polarizability [25]

$$\alpha(\delta) = -\frac{3}{4\pi^2}\epsilon_0\lambda_a^3\frac{\gamma/2}{\delta + i(\gamma+\gamma_{\rm nr})/2}. \quad (1)$$

Here, $\delta = \omega - \omega_a$, with $|\delta| \ll \omega_a$, is the detuning between the frequency of the incident light $\omega = 2\pi c/\lambda$ and that of the resonance of the particles $\omega_a = 2\pi c/\lambda_a$, and γ ($\gamma_{\rm nr}$) is the radiative (nonradiative) width of this resonance. For a closed cycling transition in atoms we have $\gamma_{\rm nr} = 0$ and the isotropic and linear response corresponds to a $J=0$ to $J=1$ transition far from saturation. The array is taken to be an infinite square lattice with lattice constant $a < \lambda$, spanning the xy plane at $z = 0$ [Fig. 1(a)]. We note that our analysis can be straightforwardly generalized to other lattice geometries.

We first focus on the simplest case of a plane wave at normal incidence. The condition $a < \lambda$ guarantees that only a single diffraction order is present in the far field such that the scattered field on both sides of the array consists of plane waves propagating in the z direction [Fig. 1(b)]. Figure 1(c) shows the transmission and reflection coefficients as a function of the lattice constant, computed for resonant light $\delta = 0$ and in the absence of nonradiative losses, $\gamma_{\rm nr} = 0$, using our analytical approach presented below. We observe that the array scatters strongly over a wide range of lattice constants. In particular, complete reflection (zero transmission) is observed at lattice constants $a/\lambda \approx 0.2, 0.8$. We note that the null transmission at $a/\lambda \approx 0.8$ was also recently found numerically in Ref. [18].

Let us now analyze the above situation. For $a < \lambda$ the total field can be written as

$$\mathbf{E} = [e^{ikz} + Se^{ik|z|}]\mathbf{E}_0, \quad (2)$$

where $\mathbf{E}_0$ is the amplitude of the field polarized in the xy plane, $k = \omega/c$, and S is a scattering amplitude. For $S = -1$, the transmitted field (at $z > 0$) vanishes and the corresponding perfect reflection gives rise to a standing wave for $z < 0$. The scattering amplitude is determined by the polarization $\mathbf{p}$ induced on the atoms by the incident field, which is identical for all atoms in this case. In turn, $\mathbf{p}$ is the result of multiple scattering of the incident field by all atoms in the array, and it can be characterized by an *effective polarizability* of the atoms defined by $\mathbf{p} = \alpha_e(\delta)\mathbf{E}_0$. A self-consistent solution of this multiple-scattering problem yields [26]

$$S(\delta) = i\pi\left(\frac{\lambda}{a}\right)^2\frac{\alpha_e(\delta)}{\varepsilon_0\lambda^3} = -\frac{i(\gamma+\Gamma)/2}{\delta - \Delta + i(\gamma+\gamma_{\rm nr}+\Gamma)/2}. \quad (3)$$

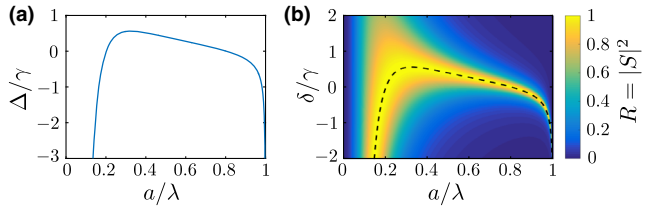

FIG. 2. (a) The cooperative shift Δ, Eq. (4), as a function of the lattice constant a (normal incidence). This plot is central in the design of the scattering since the shift determines the collective resonances of the array according to Eq. (3). Perfect reflection occurs when the cooperative shift equals the incident detuning, $\delta = \Delta$. For example, $\Delta = 0$ at $a/\lambda \approx 0.2$, 0.8 explains the resonances in Fig. 1(c). (b) Intensity reflection coefficient R as a function of lattice constant a and detuning δ. We note that the emerging contour of perfect reflection (bright yellow) coincides with the cooperative resonance plotted in (a) (marked here by the dashed black curve).

By comparing the structure of this linear response to that of an individual atom, Eq. (1), we infer that the dipolar interaction between atoms in the array renormalize both the width γ and the resonant frequency ω_a. They are now supplemented by their cooperative counterparts Γ and Δ, respectively, given by

$$\Delta - \frac{i}{2}\Gamma = -\frac{3}{2}\gamma\lambda\sum_{n\neq 0}G(0,\mathbf{r}_n), \quad \Gamma = \gamma\frac{3}{4\pi}\left(\frac{\lambda}{a}\right)^2 - \gamma. \quad (4)$$

Here, $G(0,\mathbf{r}_n)$ is the transverse component (xx or yy) of the dyadic Green's function of electrodynamics in free space [34], evaluated between the central atom ("$n = 0$") at $\mathbf{r}_0 = 0$ and the atom n at $\mathbf{r}_n$. The explicit expression for Γ holds for $a < \lambda$ and is in fact valid for *any* 2D lattice [26].

Equation (3) reveals that scattering is strongest when the frequency of the incident light matches the cooperative resonance, $\delta = \Delta$. Perfect reflection ($S = -1$) occurs if, additionally, $\gamma_{\rm nr} = 0$. Therefore, the *key ingredient* that determines the scattering properties of the array is the cooperative dipole-dipole shift Δ, given by the summation (readily evaluated numerically) of the dispersive dipole-dipole shift over all atoms, the real part of Eq. (4). Figure 2(a) provides us with a central tool by which to understand and design the scattering off the array, as it presents the cooperative shift Δ as a function of the lattice constant a [26]. For example, the vanishing cooperative shift Δ at $a/\lambda \approx 0.2$, 0.8 explains the perfect reflection obtained in Fig. 1(c) for $\delta = 0$. Moreover, Fig. 2(a) shows that scattering resonances exist for a wide range of incident field detunings δ near the individual-atom resonance. This is illustrated by Fig. 2(b), in which the reflection coefficient is plotted as a function of both a and δ.

For lossy particles, where $\gamma_{\rm nr} \neq 0$, the scattering amplitude (3) at resonance becomes $S = -(\Gamma+\gamma)/(\Gamma+\gamma+\gamma_{\rm nr})$. Therefore, high reflection requires that radiation damping via scattering is dominant over all other damping sources,

$\gamma + \Gamma \gg \gamma_{\rm nr}$. The scaling $\gamma + \Gamma \propto (\lambda/a)^2$, originating from cooperative enhancement, then implies that this can be achieved for a sufficiently small lattice constant even if the individual dipoles are poor radiators ($\gamma < \gamma_{\rm nr}$).

General angle of incidence.—The foregoing analysis can be generalized to all incident angles. We begin by considering $a < \lambda/2$, which ensures a single diffraction order for all incident plane waves, $\mathbf{E}_{0,\mathbf{k}_\parallel} e^{i\mathbf{k}_\parallel\cdot\mathbf{r}} e^{ik_z z}$, at any angle. Here $\mathbf{k}_\parallel = (k_x, k_y, 0)$ denotes the projection of the incident wave vector $\mathbf{k}$ onto the xy plane and $\mathbf{E}_{0,\mathbf{k}_\parallel}$ can be decomposed into the two possible transverse polarizations $\mathbf{e}^+_{p,s} \perp \mathbf{k}$. The total field has the form of Eq. (2), where the scattering amplitude now becomes a 3×3 matrix, and with $e^{i\mathbf{k}_\parallel\cdot\mathbf{r}_\parallel}\mathbf{E}_{0,\mathbf{k}_\parallel}$ and k_z replacing $\mathbf{E}_0$ and k, respectively. The scattering amplitude is again determined by the polarization of the atoms, which is spatially modulated by the in-plane incident wave vector, according to Bloch's theorem. The polarization of atom n can thus be written as $\mathbf{p}_n = \mathbf{p}(\mathbf{k}_\parallel) e^{i\mathbf{k}_\parallel\cdot\mathbf{r}_n}$, where

$$\mathbf{p}(\mathbf{k}_\parallel) = \overline{\overline{\alpha}}_e(\mathbf{k}_\parallel)\mathbf{E}_{0,\mathbf{k}_\parallel} \tag{5}$$

denotes the polarization in momentum space. Hence, the effective polarizability is generally defined as the linear response of the polarization of the array in momentum space, given by the tensor

$$\overline{\overline{\alpha}}_e(\mathbf{k}_\parallel) = -\frac{3}{4\pi^2}\varepsilon_0\lambda^3 \frac{\gamma/2}{\delta - \overline{\overline{\Delta}}(\mathbf{k}_\parallel) + i[\gamma + \gamma_{\rm nr} + \overline{\overline{\Gamma}}(\mathbf{k}_\parallel)]/2}. \tag{6}$$

In analogy with Eqs. (1) and (3), $\overline{\overline{\Delta}}(\mathbf{k}_\parallel)$ and $\overline{\overline{\Gamma}}(\mathbf{k}_\parallel)$ are the cooperative resonance and width tensors, respectively, given in terms of the dyadic Green's function $\overline{\overline{G}}$ by

$$\overline{\overline{\Delta}}(\mathbf{k}_\parallel) - \frac{i}{2}\overline{\overline{\Gamma}}(\mathbf{k}_\parallel) = -\frac{3}{2}\gamma\lambda \sum_{n\neq 0} \overline{\overline{G}}(0, \mathbf{r}_n) e^{i\mathbf{k}_\parallel\cdot\mathbf{r}_n}. \tag{7}$$

An analytic expression can be obtained for $\overline{\overline{\Gamma}}$ [26], while $\overline{\overline{\Delta}}$ has been evaluated numerically.

The scattering amplitude is related to the effective polarizability by an expression similar to that in Eq. (3), from which we can deduce the intensity reflection and transmission coefficients. As illustrated in Fig. 3(a) for s-polarized light, we find that the perfect reflection revealed at cooperative resonance for normal incidence, persists almost completely for all incident angles and both s and p polarizations, well beyond the paraxial regime [26]. This implies that the mirror should operate well for realistic finite size incident beams and arrays, which was further verified for Gaussian beams by a direct numerical approach [26]. The high reflection at oblique angles may again be understood in terms of cooperative resonances of the atom array. For example, in Fig. 3(b) we plot the ss matrix element of $\overline{\overline{\Delta}}$, which is seen to vary by less than an atomic linewidth over all incident angles, thus explaining the excellent reflection of s-polarized light.

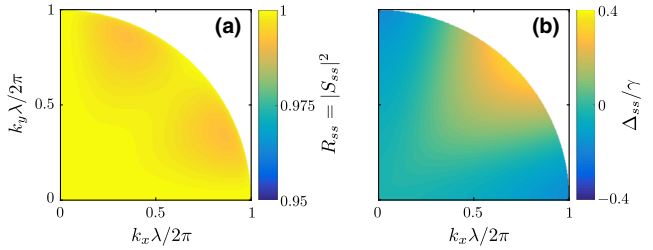

FIG. 3. Scattering at a general angle of incidence for a lattice constant $a = 0.2\lambda$. (a) Intensity reflection coefficient R_{ss} for s-polarized incident and scattered fields at zero detuning from the bare atomic resonance ($\delta = 0$) as a function of the in plane components $k_{x,y}$ of the incident wave vector. (b) ss component of the cooperative shift matrix $\overline{\overline{\Delta}}$. The variation of the energy shift around the resonance $\Delta_{ss} = \delta = 0$ is small compared to an atomic linewidth, which explains the high reflection R_{ss} at all angles.

When the lattice constant exceeds $\lambda/2$, an additional diffraction order can appear. This situation can be analyzed by a straightforward extension of the above formalism, entailing new possibilities such as retroreflection [26].

Surface dipole excitations.—More insight into the physics of the array is gained by noting that the cooperative shift $\overline{\overline{\Delta}}(\mathbf{k}_\parallel)$ describes the dispersion relation of collective surface dipole excitations. The nature of these surface modes is revealed by Eq. (5) as the normal modes of the atomic dipoles on the surface, $\mathbf{p}(\mathbf{k}_\parallel)$. The resonant frequencies of the modes and their corresponding polarizations can be deduced from their linear response $\overline{\overline{\alpha}}_e(\mathbf{k}_\parallel)$ in Eq. (6) as the three eigenvalues and eigenvectors of $\overline{\overline{\Delta}}(\mathbf{k}_\parallel)$. This interpretation also follows from the quantum master equation governing the dynamics of the atoms, wherein the eigenvalues of $\overline{\overline{\Delta}}(\mathbf{k}_\parallel)$ arise naturally as the energies of the Bloch modes of atomic excitations [26]. By diagonalizing $\overline{\overline{\Delta}}$ for each $\mathbf{k}_\parallel$ within the Brillouin zone $k_x, k_y \in [-\pi/a, \pi/a]$, we obtain the band structure of the surface modes shown in Fig. 4(a). The modes around the center of the Brillouin zone (Γ), between the vertical dotted lines, satisfy $|\mathbf{k}_\parallel| < 2\pi/\lambda$ and couple to far-field radiation. Therefore, these modes are responsible for the scattering and high reflection discussed above. In contrast, modes with $|\mathbf{k}_\parallel| > 2\pi/\lambda$ (beyond the vertical dotted lines) cannot couple to the far field, satisfying $\overline{\overline{\Gamma}} + \gamma = 0$, and are confined to the surface.

Additional possibilities to control the propagation of light are allowed via *spatial variations* in the 2D atomic array, in analogy to its macroscopic metasurface counterpart. One important example involves the design of a highly directed emission pattern from a single impurity atom coupled to the array. This can be achieved by first analyzing the coupling of the impurity atom to the surface modes, and then introducing a proper spatial modulation to the array,

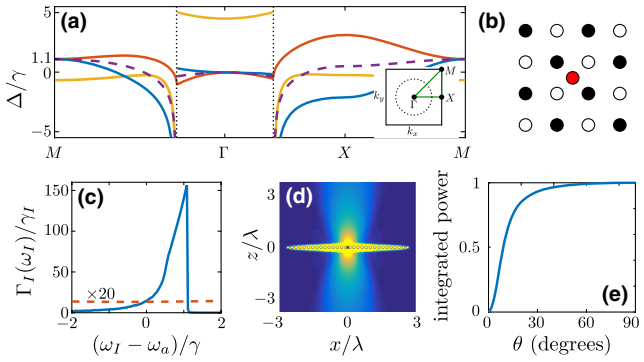

FIG. 4. (a) Band structure of the collective surface modes of the atom array for $a = 0.2\lambda$. The three bands in solid lines correspond to the three eigenvalues of the cooperative shift $\overline{\overline{\Delta}}(\mathbf{k}_\parallel)$, whereas the single dashed band is that of array atoms with a single circularly polarized transition, $\mathbf{e}_0 = (1, i, 0)/\sqrt{2}$. The inset shows the location of the special points Γ, X, M in the first Brillouin zone. The dotted vertical lines (main figure) and the circle (inset) indicate the light cone $|\mathbf{k}_\parallel| = 2\pi/\lambda$. (b) An impurity atom (red) is placed at the center of the array. The black and white colors of the array atoms represent the two sublattices which form the surface mode M. (c) Decay rate to surface modes inside (dashed) and outside (solid) the light cone, of the impurity atom with polarization $\mathbf{e}_I = (1, -i, 0)/\sqrt{2}$ as a function its transition frequency ω_I. (d) Intensity of the electric field produced by an impurity (red dot), driven at detuning $(\omega - \omega_a)/\gamma = 1.1$ and resonant with the surface modes near the corner of the Brillouin zone (M). An alternating periodic potential, $\delta\omega/\gamma = \pm 0.1$, is applied on an array of 30×30 atoms (white circles), with all other parameters the same as in (b). The bright yellow region near $z = 0$ corresponds to the excited surface modes, which are then coupled into the collimated beam by the periodic potential. (e) Emitted power integrated over a cone of half angle θ for the situation described in (d).

which selectively couples the impurity to a well-collimated, effectively 1D mode.

The decay of an excited impurity atom placed in proximity of the array [Fig. 4(b)] is strongly modified at the cooperative resonance, allowing, e.g., for the excitation of confined surface modes. Assuming, for simplicity, an array of atoms with a single dipolar transition (polarizability) in the direction $\mathbf{e}_0$, the dispersion of the surface modes can be described by a single band $\Delta(\mathbf{k}_\parallel) = \mathbf{e}_0^\dagger \overline{\overline{\Delta}}(\mathbf{k}_\parallel)\mathbf{e}_0$ [Fig. 4(a), dashed curve]. Within the Born-Markov approximation, the spontaneous emission rate from the impurity atom, with a dipole transition of frequency ω_I, orientation $\mathbf{e}_I$, and free-space radiative width $\gamma_I < \gamma$, is given by $\Gamma_I(\omega_I) = 3\gamma_I\lambda \mathrm{Im}[\mathbf{e}_I \cdot \mathbf{G}_A(\mathbf{r}_I, \mathbf{r}_I)]$ [34]. Here, $\mathbf{G}_A(\mathbf{r}, \mathbf{r}_I)$ is the electric field produced by a dipole at position $\mathbf{r}_I$, frequency ω_I and polarization $\mathbf{e}_I$, which is found, in the presence of the array, using the above formalism [35]. The emission can be decomposed into two contributions: emission into scattering modes ($|\mathbf{k}_\parallel| < 2\pi/\lambda$) and into modes confined to the surface ($|\mathbf{k}_\parallel| > 2\pi/\lambda$). Its dependence on the impurity's frequency, plotted in Fig. 4(c), exhibits a discontinuity at $(\omega_I - \omega_a)/\gamma \approx 1.1$, for the given parameters, where emission to the confined modes largely dominates over those scattered to the far field. This discontinuity arises from the resonant excitation of an extremum of the dispersion, corresponding to the surface mode $\mathbf{k}_\parallel^M = (\pi/a, \pi, a)$ on the corner of the Brillouin zone (point M) with $\Delta(\mathbf{k}_\parallel^M)/\gamma \approx 1.1$. Then, by choosing the impurity transition such that $(\omega_I - \omega_a)/\gamma = 1.1$, the emitted photon is almost entirely confined to propagate along the surface as a polariton with momentum $\mathbf{k}_\parallel^M$.

The mechanism by which this surface polariton can be outcoupled to far-field radiation can be understood as follows. The subradiant mode $\mathbf{k}_\parallel^M$ can be thought of as being formed of two degenerate dipolar sublattices of opposite phases, which destructively interfere at the far field [Fig. 4(b)]. Consider now a weak periodic potential which detunes the atoms in the array by $\pm\delta\omega$, where the sign is opposite for any two nearest-neighbor atoms. Such a perturbation splits the degeneracy between the two uniform sublattices, thus allowing them to radiate into a collimated far-field beam. Alternatively, this perturbation can be seen as a spatial modulation of the array structure containing the momentum components $(\pm\pi/a, \pm\pi/a)$, which couple the corner of the Brillouin zone (M) to the center, thus allowing for excitations at $\mathbf{k}_\parallel^M$ to be emitted into a well-defined beam normal to the array. Indeed, the numerical simulations for a finite array in Figs. 4(d), 4(e) confirm that the resulting emission is strongly collimated, with $> 90\%$ of the power emitted into a cone of half angle 25°.

Discussion.—The current study demonstrates that the scattering properties of light off a 2D atomic array are determined by the dipolar interactions between the atoms and, in particular, the cooperative resonances.

Possible experimental realizations of the 2D array include ultracold atoms trapped in either red or blue detuned optical lattices [16,36], arrays of plasmonic nanoparticles [2,4], or 2D semiconductors such as monolayers of transition metal dichalcogenides [37], where a lattice structure for the excitons or trions can be created [39–41] (see also Ref. [42]). Considering *disorder* in any of these realizations, we show in Ref. [26] that the cooperative resonances are robust to fluctuations in the atomic positions when the fluctuations are much smaller than the lattice period.

The above results suggest the potential use of such 2D arrays as powerful platforms for classical and quantum optics. In particular, the demonstrated coupling of an emitter to a collimated mode is analogous to efficient coupling to 1D photonic systems. Therefore, it should allow to obtain optical nonlinearities down to a single photon level for properly collimated incident beams [8,13–15,43–46]. Furthermore, the generalization of our approach to other nonhomogeneous arrays may allow to create "atomic-scale metasurfaces" with desired properties. Our work also opens up new prospects in optomechanics. Since the atoms are

very light but at the same time collectively exhibit nearly perfect reflection, they form a highly mechanically susceptible mirror, potentially very useful for the exploration of optomechanics at the quantum level [47].

Finally, we stress the universality of our approach, based on summation of Green's functions at lattice points, relevant for cooperative resonances at any physical system of waves and dipolelike scatterers.

We thank János Perczel for insightful comments concerning the quantum description and dispersion relation of the array. We also acknowledge valuable discussions with Vladimir Shalaev, Markus Greiner, Peter Zoller, Darrick Chang, Hongkun Park, Alex High, and Kristiaan de Greve, and financial support from NSF and the MIT-Harvard Center for Ultracold Atoms.

[1] T. W. Ebbesen, H. J. Lezec, H. F. Ghaemi, T. Thio, and P. A. Wolff, Nature (London) **391**, 667 (1998).
[2] F. J. García de Abajo, Rev. Mod. Phys. **79**, 1267 (2007).
[3] S. Xiao and N. A. Mortensen, Opt. Lett. **36**, 37 (2011).
[4] S. Thongrattanasiri, F. H. L. Koppens, and F. J. García de Abajo, Phys. Rev. Lett. **108**, 047401 (2012).
[5] S. D. Jenkins and J. Ruostekoski, Phys. Rev. Lett. **111**, 147401 (2013).
[6] N. Yu and F. Capasso, Nat. Mater. **13**, 139 (2014).
[7] A. V. Kildishev, A. Boltasseva, and V. M. Shalaev, Science **339**, 1232009 (2013).
[8] D. E. Chang, A. S. Sørensen, E. A. Demler, and M. D. Lukin, Nat. Phys. **3**, 807 (2007).
[9] J.-T. Shen and S. Fan, Phys. Rev. Lett. **98**, 153003 (2007).
[10] A. Asenjo-Garcia, J. D. Hood, D. E. Chang, and H. J. Kimble, arXiv:1606.04977.
[11] N. V. Corzo, B. Gouraud, A. Chandra, A. Goban, A. S. Sheremet, D. V. Kupriyanov, and J. Laurat, Phys. Rev. Lett. **117**, 133603 (2016).
[12] H. L. Sørensen, J.-B. Béguin, K. W. Kluge, I. Iakoupov, A. S. Sørensen, J. H. Müller, E. S. Polzik, and J. Appel, Phys. Rev. Lett. **117**, 133604 (2016).
[13] T. G. Tiecke, J. D. Thompson, N. P. de Leon, L. R. Liu, V. Vuletić, and M. D. Lukin, Nature (London) **508**, 241 (2014).
[14] I. Shomroni, S. Rosenblum, Y. Lovsky, O. Bechler, G. Guendelman, and B. Dayan, Science **345**, 903 (2014).
[15] A. Sipahigil, R. E. Evans, D. D. Sukachev, M. J. Burek, J. Borregaard, M. K. Bhaskar, C. T. Nguyen, J. L. Pacheco, H. A. Atikian, C. Meuwly, R. M. Camacho, F. Jelezko, E. Bielejec, H. Park, M. Lončar, and M. D. Lukin, Science **354**, 847 (2016).
[16] I. Bloch, Nat. Phys. **1**, 23 (2005).
[17] H. Labuhn, D. Barredo, S. Ravets, S. de Léséleuc, T. Macrì, T. Lahaye, and A. Browaeys, Nature (London) **534**, 667 (2016).
[18] R. J. Bettles, S. A. Gardiner, and C. S. Adams, Phys. Rev. Lett. **116**, 103602 (2016).
[19] J. Pellegrino, R. Bourgain, S. Jennewein, Y. R. P. Sortais, A. Browaeys, S. D. Jenkins, and J. Ruostekoski, Phys. Rev. Lett. **113**, 133602 (2014).
[20] S. D. Jenkins and J. Ruostekoski, Phys. Rev. A **86**, 031602(R) (2012).
[21] K. Kemp, S. J. Roof, M. D. Havey, I. M. Sokolov, and D. V. Kupriyanov, arXiv:1410.2497.
[22] M. O. Scully and A. A. Svidzinsky, Science **328**, 1239 (2010).
[23] R. T. Sutherland and F. Robicheaux, Phys. Rev. A **94**, 013847 (2016).
[24] K. Kempa, R. Ruppin, and J. B. Pendry, Phys. Rev. B **72**, 205103 (2005).
[25] P. Lambropoulos and D. Petrosyan, *Fundamentals of Quantum Optics and Quantum Information* (Springer, New York, 2007).
[26] See Supplemental Material at http://link.aps.org/supplemental/10.1103/PhysRevLett.118.113601 for more details, which includes Refs. [27–33].
[27] D. P. Craig and T. Thirunamachandran, *Molecular Quantum Electrodynamics* (Academic Press, London, 1984).
[28] M. O. Scully and M. S. Zubairy, *Quantum Optics* (Cambridge University Press, Cambridge, England, 1997).
[29] R. H. Lehmberg, Phys. Rev. A **2**, 883 (1970).
[30] M. Kiffner, M. Macovei, J. Eversb, and C. H. Keitel, Prog. Opt. **55**, 85 (2010).
[31] P. de Vries, D. V. van Coevorden, and A. Lagendijk, Rev. Mod. Phys. **70**, 447 (1998).
[32] J. A. Klugkist, M. Mostovoy, and J. Knoester, Phys. Rev. Lett. **96**, 163903 (2006).
[33] M. Antezza and Y. Castin, Phys. Rev. A **80**, 013816 (2009).
[34] L. Novotny and B. Hecht, *Principles of Nano-Optics* (Cambridge University Press, Cambridge, England, 2006).
[35] $\mathbf{G}_A(\mathbf{r}, \mathbf{r}_I)$ is given by the solution for $\mathbf{E}(\mathbf{r})$, with the incident field $\mathbf{E}_0(\mathbf{r})$ being the field produced by the impurity in free-space.
[36] T. Kinoshita, T. Wenger, and D. S. Weiss, Science **305**, 1125 (2004).
[37] Q. H. Wang, K. Kalantar-Zadeh, A. Kis, J. N. Coleman, and M. S. Strano, Nat. Nanotechnol. **7**, 699 (2012).
[39] H. Li, A. W. Contryman, X. Qian, S. Moeini Ardakani, Y. Gong, X. Wang, J. M. Weisse, C. H. Lee, J. Zhao, P. M. Ajayan, J. Li, H. C. Manoharan, and X. Zheng, Nat. Commun. **6**, 7381 (2015).
[40] C. Palacios-Berraquero, D. M. Kara, A. R.-P. Montblanch, M. Barbone, P. Latawiec, D. Yoon, A. K. Ott, M. Loncar, A. C. Ferrari, and M. Atatüre, arXiv:1609.04244.
[41] Y. Lin, X. Ling, L. Yu, S. Huang, A. L. Hsu, Y.-H. Lee, J. Kong, M. S. Dresselhaus, and T. Palacios, Nano Lett. **14**, 5569 (2014).
[42] S. Zeytinoglu, C. Roth, S. Huber, and A. Imamoğlu, arXiv:1701.08228.
[43] E. Vetsch, D. Reitz, G. Sagué, R. Schmidt, S. T. Dawkins, and A. Rauschenbeutel, Phys. Rev. Lett. **104**, 203603 (2010).
[44] A. Goban, C.-L. Hung, S.-P. Yu, J. D. Hood, J. A. Muniz, J. H. Lee, M. J. Martin, A. C. McClung, K. S. Choi, D. E.

Chang O. Painter, and H. J. Kimble, Nat. Commun. **5**, 3808 (2014).

[45] J. D. Thompson, T. G. Tiecke, N. P. de Leon, J. Feist, A. V. Akimov, M. Gullans, A. S. Zibrov, V. Vuletić, and M. D. Lukin, Science **340**, 1202(2013).

[46] M. Arcari, I. Söllner, A. Javadi, S. Lindskov Hansen, S. Mahmoodian, J. Liu, H. Thyrrestrup, E. H. Lee, J. D. Song, S. Stobbe, and P. Lodahl, Phys. Rev. Lett. **113**, 093603 (2014).

[47] M. Aspelmeyer, T. J. Kippenberg, and F. Marquardt, Rev. Mod. Phys. **86**, 1391 (2014).

[48] A. Srivastava, M. Sidler, A. V. Allain, D. S. Lembke, A. Kis, and A. Imamoğlu, Nat. Nanotechnol. **10**, 491 (2015).